

Relativistic Dynamics of Relative Motions (I): Post-Newtonian Extension of the Hill-Clohessy-Wiltshire Equations

Peng Xu^a

Academy of Mathematics and Systems Science,

Chinese Academy of Sciences, Beijing, 100190, China

Li-E Qiang^b

Chang'an University, Xi'an, 710054, China

With continuous advances in technologies related to deep space ranging and satellite gravity gradiometry, corrections from general relativity to the dynamics of relative orbital motions will certainly become important. In this work, we extend, in a systematic way, the Hill-Clohessy-Wiltshire Equations to include the complete first order post-Newtonian effects from general relativity. Within certain short time limit, post-Newtonian corrections to general periodic solutions of the Hill-Clohessy-Wiltshire Equations are also worked out.

I. Introduction and Motivations

The studies of relative motions between orbiting satellites can date back to early 1960s, which, by then, was motivated mainly by the satellites rendezvous problem. Clohessy and Wiltshire in their celebrated work [1] analyzed the motion of a satellite with respect to a reference one that following a circular orbit around an uniform and spherical gravitational source. With the assumption that the distance between the two satellites is short compared with the orbital radius, the system of

^a Research Associate, Institute of Applied Mathematics, xupeng@amss.ac.cn

^b Lecturer, Department of Geophysics, College of the Geology Engineering and Geomatics, qqllee815@chd.edu.cn

linear equations around the null solutions, that the so-called Clohessy-Wiltshire equations, were derived. Such equations are also known as Hill's equations, since Hill had employed the same method to study the motions of the Moon with respect to the Sun-Earth system [2]. The Hill-Clohessy-Wiltshire (HCW) equations and the related methods had then found wide applications. In-depth analysis including nonlinear effects, eccentricity, central source oblateness, drags, and other perturbations had also been carried out.

The HCW equations had proved useful to satellite geodesy, such as to the error analysis of satellite altimetry [3], computations of the ephemerides of GPS orbits [4], and the analysis of low-flying Earth orbiters [5, 6]. In the pioneering work of Wolff [7], it was pointed out that the global variations and intensities of the Earth geopotentials could be mapped out given the range and range rate data of a Satellite-to-Satellite Tracking (SST) system. Based on such principle, the Gravity Recovery and Climate Experiment (GRACE) mission had continuously provided us valuable data through its microwave inter-satellites range measurements in the past 14 years. To continue the measurements of the Earth geopotential variations, NASA had scheduled the launch of the GRACE Follow On mission, which will be supplemented with a laser interferometer of nanometer-level accuracy. GRACE II and other possible Next Generation Gravity Missions (NGGM) are also under investigations. The HCW equations had played an important part in the pre-mission analysis and the gravity field determinations of such SST missions [8–10]. Based on the HCW equations, the so called semi-analytic method of gravity field analysis from satellite observations had also been developed [11]. With the continuous advances in technologies related to deep space ranging, especially the laser interferometry in space, the sensitivities and resolutions of NGGMs that based on measurements of inter-satellites ranges or distances between orbiting proof masses will be greatly improved. Therefore, general relativistic corrections from spacetime curvature to the dynamics of relative orbital motions will certainly become important and can not be ignored.

As an example, the LISA PathFinder (LPF) mission [12] carried two proof masses that were successfully put in pure gravitational free fall with acceleration noise maintained to $5.2 \pm 0.1 \text{ fm/s}^2 \sqrt{Hz}$ in the frequency band $0.7 \text{ mHz} \sim 20 \text{ mHz}$, and its on-board laser interferometer as the readout of the relative motions between the proof masses had the sensitivity better than $9 \text{ pm}/\sqrt{Hz}$ in

the same band. The measurement scheme of the LPF can be viewed as a demonstration of an one-dimensional optical gravity gradiometer, and its success may pave the way of applying high-precision optical gradiometers in future gravity missions (e.g. the geo-Q mission). With such high sensitivities, the advantage of using orbiting optical gradiometer in relativistic experiments are now under investigations [13]. Also, for SST missions like the GRACE, it is known that certain effects from General Relativity (GR) need to be considered (numerically) in data analysis. And, it had been noticed that tests of relativistic gravitational theories may be carried out with the observations from the GRACE Follow On [15] and future satellite gravity gradiometry missions [16–18]. Therefore, to provide the theoretical tools, it is meaningful to generalize, in a systematic and self-consistence way, the HCW analysis of relative motions to include corrections from GR.

In the next section, a systematic approach, through the (Jacobi) geodesic deviation equation, of analyzing the linearized dynamics of relative motions between orbiting satellites or proof masses in GR is explained in a self-contained manner. With models and notations introduced, from Sec. III to V, we derive the generalized HCW equations including the complete first order Post-Newtonian (PN) [19, 20] effects from GR under the conditions of weak fields and slow motions in Solar system. Within certain short time limit, the general PN corrections to periodic solutions of the classical HCW equations are worked out analytically.

II. Linearized Dynamics of Relative Motions in GR

Einstein’s general theory of relativity is a geometric theory of gravitation. In the past few decades, the fundamental principle, that the Einstein’s equivalence principle, behind such geometric theory and the many critical predictions drawn from GR (including gravitational waves [21]) had been well-tested with great accuracies [20, 22]. Today, GR is still the best fit relativistic theory of gravitation among the many alternatives [20].

In GR, satellites or proof masses freely falling in gravitational field will follow geodesic world lines in a 4-dimensional spacetime, which extremize the action (length of world lines)

$$S = \int \sqrt{-g_{\mu\nu}\tau^\mu\tau^\nu} d\tau \quad (1)$$

where $g_{\mu\nu}$ is the spacetime metric field, $\tau^\mu = dx^\mu/d\tau$ the 4-velocity of the satellite or proof mass

and τ the proper time measured along the world line. In this work, we use $i, j, k, \dots = 1, 2, 3$ to index the spatial tensor components and $\mu, \nu, \lambda, \dots = 0, 1, 2, 3$ the spacetime tensor components, and the Einstein summation convention is assumed. For Solar system experiments, the typical speed v of orbiting satellites is much smaller compared with the speed of light c , especially for low or medium Earth orbits the ratio $v/c = \epsilon$ is about $10^{-5} \sim 10^{-6}$. Also, according to the Virial theorem for Newtonian system, one has $v^2/c^2 \sim U/c^2 \sim \mathcal{O}(\epsilon^2)$, where U is the Newtonian potential and the dimensionless quantity U/c^2 is a measure of the strength of the gravitational field. Therefore, Newtonian gravity can be viewed as the weak field and slow motion approximation of GR up to $\mathcal{O}(\epsilon^2)$. For satellite gravity missions and space-borne relativistic experiments in the present-day and near future, it is sufficient to keep the (dimensionless) working precision up to $\mathcal{O}(\epsilon^4)$, which just gives rise to the Post-Newtonian approximation of GR [19, 20]. For clarity, the geometric units $G = c = 1$ are adopted hereafter, and in Sec. V the SI units will be recovered. The action in Eq.(1) may be expanded as

$$\begin{aligned}
S &= \int \sqrt{-g_{00} \left(\frac{dx^0}{d\tau} \right)^2 - 2g_{0i} \frac{dx^0}{d\tau} \frac{dx^i}{d\tau} - g_{ij} \frac{dx^i}{d\tau} \frac{dx^j}{d\tau}} d\tau \\
&\sim \int \sqrt{-g_{00} - 2g_{0i} v^i - g_{ij} v^i v^j} d\tau \\
&\sim \int \sqrt{-g_{00} - 2g_{0i} \mathcal{O}(\epsilon) - g_{ij} \mathcal{O}(\epsilon^2)} d\tau.
\end{aligned} \tag{2}$$

Therefore, to study geodesic or orbit motions up to the PN level the metric components have to be expanded to

$$g_{00} \sim -1 + \mathcal{O}(\epsilon^4), \quad g_{0i} \sim \mathcal{O}(\epsilon^3), \quad g_{ij} \sim 1 + \mathcal{O}(\epsilon^2). \tag{3}$$

In this work, we model Earth as an ideal uniform and rotating spherical body, with total mass M and angular momentum \vec{J} . The inertia and geocentric Cartesian coordinates system $\{t, x^i\}$ is chosen that one of its spatial basis $\frac{\partial}{\partial x^3}$ is parallel to the direction of \vec{J} and the coordinate time t is measured by observers in the asymptotically flat region. According to Eq. (3), the PN metric

outside Earth may be expanded as [23, 24]

$$g_{\mu\nu} = \begin{pmatrix} -1 + 2U - 2U^2 & \frac{2x^2 J}{r^3} & -\frac{2x^1 J}{r^3} & 0 \\ \frac{2x^2 J}{r^3} & 1 + 2U & 0 & 0 \\ -\frac{2x^1 J}{r^3} & 0 & 1 + 2U & 0 \\ 0 & 0 & 0 & 1 + 2U \end{pmatrix}, \quad (4)$$

where $r = \sqrt{(x^1)^2 + (x^2)^2 + (x^3)^2}$. The PN order relations for an orbiting satellite or proof mass read

$$v^2 \sim \frac{M}{r} \sim \mathcal{O}(\epsilon^2), \quad (5)$$

$$v^4 \sim \frac{M^2}{r^2} \sim \frac{Jv}{r^2} \sim \mathcal{O}(\epsilon^4). \quad (6)$$

Deviations from uniform sphere of the centered gravitational source will give rise to corrections to the above metric, and their main contributions will be the geopotential multipoles (in terms of the spherical harmonics) added to the Newtonian potential U in the time-time component of the metric

$$g_{00} = -1 + 2\frac{M}{r} \left(1 + \sum_{l=2}^{\infty} \left(\frac{R}{r}\right)^l \sum_{m=-l}^l C_{lm} Y_{lm}\right) - \frac{2M^2}{r^2}, \quad (7)$$

where R is the averaged radius of Earth. While, since J_2 is a rather large component, which is only about 4×10^{-4} times smaller than the monopole field $\frac{M}{r}$ of Earth. Therefore, considering the possible sensitivities and resolutions for future gravity missions, the relativistic corrections from J_2 should also be included and the more accurate metric turns out to be

$$g_{\mu\nu} = \begin{pmatrix} -1 + \frac{2M}{r} \left(1 + \sum_{l=2}^{\infty} \left(\frac{R}{r}\right)^l \sum_{m=-l}^l C_{lm} Y_{lm}\right) - \frac{2M^2}{r^2} - \frac{4C_{20}R^2M^2}{r^4} Y_{20} & \frac{2x^2 J}{r^3} & -\frac{2x^1 J}{r^3} & 0 \\ \frac{2x^2 J}{r^3} & 1 + 2\left(\frac{M}{r} + \frac{C_{20}R^2M}{r^3} Y_{20}\right) & 0 & 0 \\ -\frac{2x^1 J}{r^3} & 0 & 1 + 2\left(\frac{M}{r} + \frac{C_{20}R^2M}{r^3} Y_{20}\right) & 0 \\ 0 & 0 & 0 & 1 + 2\left(\frac{M}{r} + \frac{C_{20}R^2M}{r^3} Y_{20}\right) \end{pmatrix}. \quad (8)$$

In this first-step theoretical study of the relativistic dynamics of relative motions, we will restrict ourselves to work with the metric field of the ideal Earth model given in Eq. (4). Subsequent studies

including perturbations from certain multipoles based on the metric in Eq. (8) and the possible applications to SST missions like the GRACE and GRACE Follow On, especially the effects on the measurement accuracy of the J_2 component, will be left in a separated publication.

Given the metric field, the relative motions among a family of adjacent free-falling proof masses or satellites are driven by the spacetime curvature. Especially, when the distance between the adjacent two satellites or proof masses is smaller compared with the curvature radius of the corresponding spacetime region, their relative motion satisfies the so called (Jacobi) geodesic deviation equation [25]

$$\tau^\rho \nabla_\rho \tau^\lambda \nabla_\lambda Z^\mu + R_{\rho\nu\lambda}{}^\mu \tau^\rho \tau^\lambda Z^\nu = 0, \quad (9)$$

which is evaluated along the world line of the reference satellite or mass. Here ∇_μ denotes the covariant derivative associate to the given metric, $R_{\rho\nu\lambda}{}^\mu$ the Riemann curvature tensor, and Z^μ is the position difference 4-vector (connection vector) pointing from the reference satellite or mass to the second one. This is a linear equation of the position difference Z^μ , and effects from spacetime curvature can be interpreted as tidal forces under local inertia frames (Fermi-shifted local frame [25]) carried by the reference satellite or mass, see [26] for details.

Back to our problem, the world lines in spacetime corresponding to the adjacent orbits of satellites or proof masses can be illustrated in Fig. 1. In the local frame, which is defined by the tetrad $e_{(a)}{}^\mu$ ($a = 0, 1, 2, 3$) attached to the reference satellite or mass with $e_{(0)}{}^\mu = \tau^\mu$, the above geodesic deviation equation can be expanded as

$$\begin{aligned} \frac{d^2}{d\tau^2} Z^{(a)} &= -2\gamma_{(b)(0)}^{(a)} \frac{d}{d\tau} Z^{(b)} \\ &\quad - \left(\frac{d}{d\tau} \gamma_{(b)(0)}^{(a)} + \gamma_{(b)(0)}^{(c)} \gamma_{(c)(0)}^{(a)} \right) Z^{(b)} \\ &\quad - K_{(b)}^{(a)} Z^{(b)}, \end{aligned} \quad (10)$$

where $Z^{(a)} e_{(a)}{}^\mu = Z^\mu$ and $\gamma_{(b)(c)}^{(a)} = e^{(a)\nu} \nabla_\mu e_{(b)\nu} e_{(c)}{}^\mu$ are the Ricci rotation coefficients [25]. Here $\{(a), (b), \dots\}$ and $\{(i), (j), \dots\}$ are used to index tensor components under the local frame. The first line of the right hand side of the above equation contains the relativistic analogue of the Coriolis force, the second line contains the inertia forces and the third line is the tidal force from

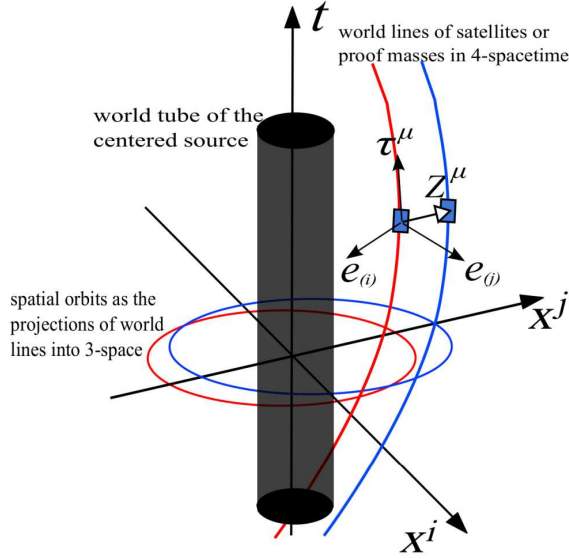


Fig. 1 The illustration of the world lines of adjacent orbiting satellites or proof masses in spacetime. The spatial orbits can be viewed as the projections of the world lines into the 3-space. The variations of the connection vector Z^μ , or the relative motions between adjacent satellites or masses, is determined by spacetime curvature.

the spacetime curvature. The tidal matrix is defined by

$$K_{\mu\nu} = R_{\rho\mu\lambda\nu} \tau^\rho \tau^\lambda, \quad (11)$$

$$K_{(a)(b)} = K_{\mu\nu} e_{(a)}^\mu e_{(b)}^\nu. \quad (12)$$

To summarize, Eq. (10) is the natural starting point to analyze the linearized dynamics of relative orbit motions in GR. As one will see, if all the relativistic effects are left out, Eq. (10) will reduce to the system of linear equations of relative motions in Newtonian gravity. In the following sections, we will evaluate Eq. (10) under the local tetrad $e_{(a)}^\mu$ along a relativistic precessing circular orbit. It is natural to choose the spatial bases $e_{(i)}^\mu$ to be the triad of the Local-Vertical-Local-Horizontal (LVLH) frame with relativistic corrections. The explicit form of the PN extension of the HCW equations is derived, and the PN corrections to the periodic solutions of the HCW equations are worked out.

III. Post-Newtonian Reference Orbit

As discussed in the last section, satellites or proof masses that moving freely in gravitational field will extremize the action given in Eq. (1), and therefore satisfy the following geodesic equation [23, 25]

$$\frac{d^2 x^\mu}{d\tau^2} + \Gamma^\mu_{\rho\lambda} \frac{dx^\rho}{d\tau} \frac{dx^\lambda}{d\tau} = 0, \quad (13)$$

where $\Gamma^\mu_{\rho\lambda}$ denotes the Christoffel symbols. Replacing the proper time τ with the coordinate time t of the geocentric coordinates system, the geodesic equation becomes

$$\begin{aligned} \frac{d^2 x^i}{dt^2} = & -\Gamma^i_{00} - 2\Gamma^i_{0j} \frac{dx^j}{dt} - \Gamma^i_{jk} \frac{dx^j}{dt} \frac{dx^k}{dt} \\ & + (\Gamma^0_{00} + 2\Gamma^0_{0j} \frac{dx^j}{dt} + \Gamma^0_{jk} \frac{dx^j}{dt} \frac{dx^k}{dt}) \frac{dx^i}{dt}. \end{aligned} \quad (14)$$

Given the PN metric in Eq. (4), the components of $\Gamma^\mu_{\rho\lambda}$ under the geocentric coordinates system can be worked out up to the required order as

$$\Gamma^0_{0\mu} = \frac{M}{r^3} \begin{pmatrix} 0 \\ x^1 \\ x^2 \\ x^3 \end{pmatrix}, \quad (15)$$

$$\Gamma^i_{0j} = \begin{pmatrix} 0 & -\frac{J((x^1)^2 + (x^2)^2 - 2(x^3)^2)}{r^5} & -\frac{3Jx^2x^3}{r^5} \\ \frac{J((x^1)^2 + (x^2)^2 - 2(x^3)^2)}{r^5} & 0 & \frac{3Jx^1x^3}{r^5} \\ \frac{3Jx^2x^3}{r^5} & -\frac{3Jx^1x^3}{r^5} & 0 \end{pmatrix}, \quad (16)$$

$$\Gamma^1_{ij} = -\frac{M}{r^3} \begin{pmatrix} x^1 & x^2 & x^3 \\ x^2 & -x^1 & 0 \\ x^3 & 0 & -x^1 \end{pmatrix}, \quad (17)$$

$$\Gamma^2_{ij} = -\frac{M}{r^3} \begin{pmatrix} -x^2 & x^1 & 0 \\ x^1 & x^2 & x^3 \\ 0 & x^3 & -x^2 \end{pmatrix}, \quad (18)$$

$$\Gamma^3_{ij} = -\frac{M}{r^3} \begin{pmatrix} -x^3 & 0 & x^1 \\ 0 & -x^3 & x^2 \\ x^1 & x^2 & x^3 \end{pmatrix}, \quad (19)$$

$$\Gamma^0_{ij} = \begin{pmatrix} \frac{6J(x^2(x^1)^3+x^2((x^2)^2+(x^3)^2)x^1)}{r^7} & \frac{3J(-(x^3)^2(x^1)^2-(x^1)^4+(x^2)^2((x^2)^2+(x^3)^2))}{r^7} & \frac{3J(x^2x^3(x^1)^2+x^2x^3((x^2)^2+(x^3)^2))}{r^7} \\ \frac{3J(-(x^3)^2(x^1)^2-(x^1)^4+(x^2)^2((x^2)^2+(x^3)^2))}{r^7} & -\frac{6J(x^2(x^1)^3+x^2((x^2)^2+(x^3)^2)x^1)}{r^7} & -\frac{3J(x^3(x^1)^3+x^3((x^2)^2+(x^3)^2)x^1)}{r^7} \\ \frac{3J(x^2x^3(x^1)^2+x^2x^3((x^2)^2+(x^3)^2))}{r^7} & -\frac{3J(x^3(x^1)^3+x^3((x^2)^2+(x^3)^2)x^1)}{r^7} & 0 \end{pmatrix}. \quad (20)$$

Substitute $\Gamma^\mu_{\rho\lambda}$ into Eq. (14) we then have the equation of motion in PN approximations

$$\frac{d^2\vec{x}}{dt^2} = \vec{f}_N + \vec{f}_{GE} + \vec{f}_{GM}, \quad (21)$$

where $\vec{f}_N = -\frac{M}{r^3}\vec{x}$ is the Newtonian force per unit mass, and the relativistic corrections may be divided into two parts that the GravitoElectric (GE) force and GravitoMagnetic (GM) force per unit mass

$$\vec{f}_{GE} = \frac{M}{r^3} \left(\left(\frac{4M}{r} - v^2 \right) \vec{x} + 4(\vec{x} \cdot \vec{v}) \vec{v} \right), \quad (22)$$

$$\vec{f}_{GM} = 2\vec{v} \times \left(\frac{\vec{J}}{r^3} - \frac{3(\vec{J} \cdot \vec{x})\vec{x}}{r^5} \right). \quad (23)$$

For detailed discussions of the analogies between electrodynamics and the linearized dynamics of GR, please consults [27–29]. Here, such a separation of the relativistic perturbations will help us in solving the PN circular orbit. Along an unperturbed Keplerian circular orbit, one notices that the PN GE force becomes a centrifugal one with constant magnitude

$$\vec{f}_{GE} = \frac{M}{r^3} \left(\frac{4M}{r} - v^2 \right) \vec{x},$$

and the projection of the GM force along the radial direction is also a constant

$$f_{GM}^r = \vec{f}_{GM} \cdot \frac{\vec{x}}{r} = 2 \frac{\vec{J} \cdot \vec{L}}{r^4},$$

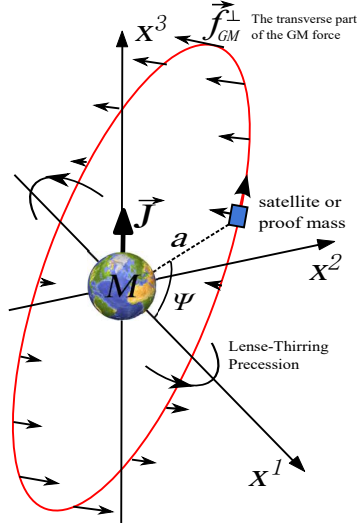


Fig. 2 The transverse part of the GM force \vec{f}_{GM}^{\perp} acting on the satellite or proof mass along a circular orbit and the Lense-Thirring precession of the orbit plane about the direction of \vec{J} .

where \vec{L} is the angular momentum of the orbiting satellite or proof mass. Thus \vec{f}_{GE} together with \vec{f}_{GM}^r will only modify the total centripetal force and therefore give rise to a relativistic correction to the mean angular frequency ω . The residual part of the PN perturbations is a periodic force \vec{f}_{GM}^{\perp} that transverse to the orbit plane, which will drive the orbit plane to precess about the direction of \vec{J} (the Lense-Thirring precession [30]), see Fig. 2 for illustration.

According to the above discussions, for the ideal case of an orbit with constant radius a , the PN perturbations of the orbital elements can be solved analytically up to the first order, therefore the nearly circular orbit that satisfying the geodesic equation (13) can be worked out to the PN level as

$$x^1 = a \cos \Psi \cos \left(\frac{2J\tau}{a^3} \right) - a \cos i \sin \Psi \sin \left(\frac{2J\tau}{a^3} \right), \quad (24)$$

$$x^2 = a \cos i \sin \Psi \cos \left(\frac{2J\tau}{a^3} \right) + a \cos \Psi \sin \left(\frac{2J\tau}{a^3} \right), \quad (25)$$

$$x^3 = a \sin i \sin \Psi, \quad (26)$$

where i denotes the inclination, $\Psi = \omega\tau$ is the true anomaly and the initial longitude of ascending node $\Omega(0)$ is set to be zero. For clarity, the time parameter is replaced back to the proper time τ measured along the above orbit, that from the differential line element $d\tau^2 = -g_{\mu\nu}dx^\mu dx^\nu$ along the orbits the ratio $\frac{dt}{d\tau}$ can be solved

$$\frac{dt}{d\tau} = 1 + \frac{a^2\omega^2}{2} + \frac{M}{a} - \frac{a^4\omega^4}{8} + \frac{3Ma\omega^2}{2} + \frac{M^2}{2a^2}. \quad (27)$$

The PN modified angular frequency with respect to τ can be worked out as

$$\omega = \sqrt{\frac{M}{a^3}} - \frac{3J \cos i}{M}. \quad (28)$$

Due to the frame-dragging effect [28], the orbit plane precesses extremely slowly with rate $\dot{\Omega}(\tau) = \frac{2J}{a^3}$ about the direction of \vec{J} . For a general low or medium Earth orbit it will take about $\frac{c^2 \pi a^3}{GJ} \sim 10^7 \text{ yrs}$ to finish one period.

We will work with the orbit given in Eq. (24)-(28) in this work. Perturbations from small eccentricities and the corresponding PN effects are left for future studies. The tidal matrix $K_{\mu\nu}$ defined in Eq. (11) along the this orbit can be worked out under the geocentric coordinates system as

$$(K^N)_{\mu\nu} = \frac{M}{a^3} \begin{pmatrix} 0 & 0 & 0 & 0 \\ 0 & -\frac{1}{2}(3 \cos 2\Psi + 1) & -\frac{3}{2} \cos i \sin 2\Psi & -\frac{3}{2} \sin i \sin 2\Psi \\ 0 & -\frac{3}{2} \cos i \sin 2\Psi & \frac{1}{4}(6 \cos 2\Psi \cos^2 i - 3 \cos 2i + 1) & -3 \cos i \sin i \sin^2 \Psi \\ 0 & -\frac{3}{2} \sin i \sin 2\Psi & -3 \cos i \sin i \sin^2 \Psi & \frac{1}{4}(6 \cos 2\Psi \sin^2 i + 3 \cos 2i + 1) \end{pmatrix}, \quad (29)$$

$$(K^{GE})_{\mu\nu} =$$

$$\frac{M}{a^3} \begin{pmatrix} a^2 \omega^2 & a \omega \sin \Psi & -a \omega \cos i \cos \Psi & -a \omega \sin i \cos \Psi \\ a \omega \sin \Psi & \frac{M}{2a}(1 + 3 \cos 2\Psi) & (\frac{3M}{2a} - 2a^2 \omega^2) \cos i \sin 2\Psi & (\frac{3M}{2a} - 2a^2 \omega^2) \sin i \sin 2\Psi \\ & -a^2 \omega^2(1 + 2 \cos 2\Psi) & & \\ -a \omega \cos i \cos \Psi & (\frac{3M}{2a} - 2a^2 \omega^2) \cos i \sin 2\Psi & -a^2 \omega^2(2 \cos 2i - 1) & + \frac{3M \sin 2i \sin^2 \Psi}{2a} \\ & & + \frac{M(-6 \cos 2\Psi \cos^2 i + 3 \cos 2i - 1)}{4a} & \\ & & a^2 \omega^2 \sin 2i(\cos 2\Psi - 2) & a^2 \omega^2 \sin 2i(\cos 2\Psi - 2) \\ -a \omega \sin i \cos \Psi & (\frac{3M}{2a} - 2a^2 \omega^2) \sin i \sin 2\Psi & + \frac{3M \sin 2i \sin^2 \Psi}{2a} & + a^2 \omega^2(2 \cos 2i + 1) \\ & & & - \frac{M(6 \cos 2\Psi \sin^2 i + 3 \cos 2i + 1)}{4a} \end{pmatrix}, \quad (30)$$

$$(K^{GM})_{\mu\nu} = \frac{3J\omega}{a^3} \begin{pmatrix} 0 & 0 & 0 & 0 \\ 0 & 2 \cos i \cos^2 \Psi & \frac{1}{2}(3 \cos 2i - 1) \sin 2\Psi & 3 \sin 2i \sin \Psi \cos \Psi \\ 0 & \frac{1}{2}(3 \cos 2i - 1) \sin 2\Psi & \cos i(5 \cos 2i - 3) \sin^2 \Psi & \frac{1}{4}(10 \sin 3i \sin^2 \Psi) \\ & & + \frac{1}{4}(3 \cos 2\Psi \sin i + \sin i) & \\ 0 & 3 \sin 2i \sin \Psi \cos \Psi & \frac{1}{4}(10 \sin 3i \sin^2 \Psi) & -\frac{1}{4} \cos i(20 \cos 2\Psi \sin^2 i + 3) \\ & & + \frac{1}{4}(3 \cos 2\Psi \sin i + \sin i) & -\frac{5}{4} \cos 3i \end{pmatrix}, \quad (31)$$

and within mission life-time T much smaller compared with the period of the Lense-Thirring pre-

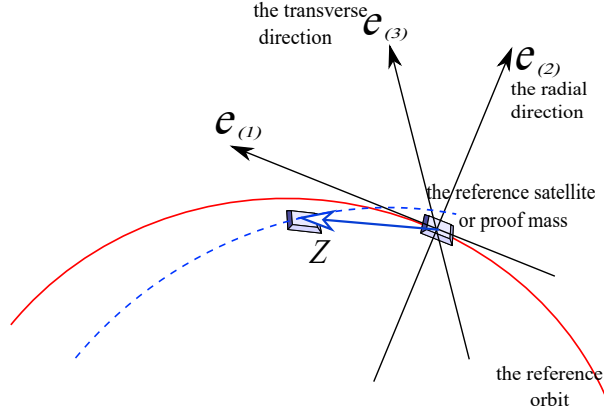


Fig. 3 The local frame attached to the reference satellite or proof mass.

cession, that $\frac{T}{a} \ll \frac{\pi a^2}{J}$, we also have

$$(K^{LT})_{\mu\nu} = \frac{3JM\Psi}{a^6\omega} \begin{pmatrix} 0 & 0 & 0 & 0 \\ 0 & 2\cos i \sin 2\Psi & -\frac{1}{2}(\cos 2i + 3)\cos 2\Psi - \sin^2 i & \sin 2i \sin^2 \Psi \\ 0 & -\frac{1}{2}(\cos 2i + 3)\cos 2\Psi - \sin^2 i & -2\cos i \sin 2\Psi & -\sin i \sin 2\Psi \\ 0 & \sin 2i \sin^2 \Psi & -\sin i \sin 2\Psi & 0 \end{pmatrix}. \quad (32)$$

Here, $K_{\mu\nu}$ is decomposed into four parts, the Newtonian part $(K^N)_{\mu\nu}$, the PN GE part $(K^{GE})_{\mu\nu}$, the GM part $(K^{GM})_{\mu\nu}$ and the secular part $(K^{LT})_{\mu\nu}$. The secular terms in $(K^{LT})_{\mu\nu}$ are in fact periodic ones with periods $\sim \frac{\pi a^3}{J}$, which are produced by the modulation of the Newtonian tidal tensor due to the Lense-Thirring precession of the orbit with respect to the geocentric coordinates system. For mission life time T about a few years with total orbital cycles $\frac{\Psi}{2\pi} \sim 10^4$, the secular tensor is of the PN level $|(K^{LT})_{\mu\nu}| \sim \frac{JMT}{a^6} \sim \frac{1}{a^2}\Psi\mathcal{O}(\epsilon^4)$.

IV. Local Frame Along Post-Newtonian Orbit

In this section, we work out the tetrad $e_{(a)}{}^\mu$ attached to the satellite or proof mass that following the orbit given in Eq. (24)-(26). The relativistic corrections up to the PN level in the tetrad need to be included.

We first set $e_{(0)}^\mu = \tau^\mu = \frac{dx^\mu}{d\tau}$, which is the 4-velocity of the reference satellite or proof mass.

Along the orbit given in Eq. (24)-(26), we have

$$e_{(0)}^\mu = \tau^\mu = \begin{pmatrix} 1 + \frac{a^2\omega^2}{2} + \frac{M}{a} \\ -a\omega \sin \Psi - \frac{2J \cos i (\sin \Psi + \Psi \cos \Psi)}{a^2} \\ a\omega \cos i \cos \Psi + \frac{2J (\cos \Psi - \Psi \sin \Psi)}{a^2} \\ a\omega \sin i \cos \Psi \end{pmatrix}. \quad (33)$$

Second, we set the orthonormal spacial triad $\vec{e}_{(i)}$ as follows, that $\vec{e}_{(1)}$ is parallel to the direction of the instance 3-velocity $\vec{v} = \frac{d\vec{x}}{dt}$ of the reference satellite or proof mass, $\vec{e}_{(2)}$ is along the radial direction \vec{x} and $\vec{e}_{(3)} = \vec{e}_{(1)} \times \vec{e}_{(2)}$, see Fig. 3 for illustration. Last but not least, since the local frame is moving along the world line of the reference satellite or proof mass, one needs to perform the boost Lorentz transformations of the triad with respect to the 4-velocity τ^μ . Within the short time limits that $\frac{\tau}{a} \ll \frac{\pi a^2}{J}$ we then have

$$e_{(1)}^\mu = \begin{pmatrix} \omega(a - M) + \frac{2J \cos i}{a^2} \\ -\left(1 - \frac{M}{a} + \frac{a^2\omega^2}{2}\right) \sin \Psi - \frac{2J\Psi \cos i \cos \Psi}{a^3\omega} \\ \left(1 - \frac{M}{a} + \frac{a^2\omega^2}{2}\right) \cos i \cos \Psi + \frac{2J \sin^2 i \cos \Psi - 2J\Psi \sin \Psi}{a^3\omega} \\ \left(1 - \frac{M}{a} + \frac{a^2\omega^2}{2}\right) \sin i \cos \Psi - \frac{2J \cos i \sin i \cos \Psi}{a^3\omega} \end{pmatrix}, \quad (34)$$

$$e_{(2)}^\mu = \begin{pmatrix} 0 \\ \left(1 - \frac{M}{a}\right) \cos \Psi - \frac{2J\Psi \cos i \sin \Psi}{a^3\omega} \\ \left(1 - \frac{M}{a}\right) \cos i \sin \Psi + \frac{2J\Psi \cos \Psi}{a^3\omega} \\ \left(1 - \frac{M}{a}\right) \sin i \sin \Psi \end{pmatrix}, \quad (35)$$

$$e_{(3)}^\mu = \begin{pmatrix} 0 \\ \frac{J \sin i (\sin 2\Psi - 2\Psi)}{a^3\omega} \\ \left(1 - \frac{M}{a} - \frac{2J \cos i \cos^2 \Psi}{a^3\omega}\right) \sin i \\ \left(-1 + \frac{M}{a}\right) \cos i - \frac{2J \sin^2 i \cos^2 \Psi}{a^3\omega} \end{pmatrix}. \quad (36)$$

Therefore, the tetrad matrix $e_{(a)}^\mu$, which can be viewed as the transformation matrix from the local

frame to the geocentric coordinates system, and its inverse $e^{(a)}_{\mu}$ can be worked out as

$$e_{(a)}^{\mu} = \begin{pmatrix} 1 + \frac{a^2\omega^2}{2} + \frac{M}{a} & -a\omega \sin \Psi & a\omega \cos i \cos \Psi & a\omega \sin i \cos \Psi \\ -\frac{2J \cos i (\Psi \cos \Psi + \sin \Psi)}{a^2} & +\frac{2J (\cos \Psi - \Psi \sin \Psi)}{a^2} & & \\ (a-M)\omega & -(1 - \frac{M}{a} + \frac{a^2\omega^2}{2}) \sin \Psi & (1 - \frac{M}{a} + \frac{a^2\omega^2}{2}) \cos i \cos \Psi & (1 - \frac{M}{a} + \frac{a^2\omega^2}{2}) \sin i \cos \Psi \\ +\frac{2J \cos i}{a^2} & -\frac{2J \Psi \cos i \cos \Psi}{a^3\omega} & +\frac{2J \sin^2 i \cos \Psi - 2J \Psi \sin \Psi}{a^3\omega} & -\frac{2J \cos i \sin i \cos \Psi}{a^3\omega} \\ 0 & (1 - \frac{M}{a}) \cos \Psi & (1 - \frac{M}{a}) \cos i \sin \Psi & (1 - \frac{M}{a}) \sin i \sin \Psi \\ & -\frac{2J \Psi \cos i \sin \Psi}{a^3\omega} & +\frac{2J \Psi \cos \Psi}{a^3\omega} & \\ 0 & \frac{J \sin i (\sin 2\Psi - 2\Psi)}{a^3\omega} & (1 - \frac{M}{a}) \sin i & (-1 + \frac{M}{a}) \cos i \\ & & -\frac{2J \sin i \cos i \cos^2 \Psi}{a^3\omega} & -\frac{2J \cos^2 \Psi \sin^2 i}{a^3\omega} \end{pmatrix}, \quad (37)$$

$$e^{(a)}_{\mu} = \begin{pmatrix} 1 + \frac{a^2\omega^2}{2} - \frac{M}{a} & -a\omega - \frac{2J \cos i}{a^2} & 0 & 0 \\ (a-M)\omega \sin \Psi & -(1 + \frac{\omega^2 a^2}{2} + \frac{M}{a}) \sin \Psi & (1 + \frac{M}{a}) \cos \Psi & -\frac{J \sin i (2\Psi - \sin 2\Psi)}{a^3\omega} \\ +\frac{2J \cos i (\Psi \cos \Psi + \sin \Psi)}{a^2} & -\frac{2J \Psi \cos i \cos \Psi}{a^3\omega} & -\frac{2J \Psi \cos i \sin \Psi}{a^3} & \\ (M-a)\omega \cos i \cos \Psi & (1 + \frac{\omega^2 a^2}{2} + \frac{M}{a}) \cos i \cos \Psi & (1 + \frac{M}{a}) \cos i \sin \Psi & (1 + \frac{M}{a}) \sin i \\ +\frac{2J (\Psi \sin \Psi - \cos \Psi)}{a^2} & +\frac{2J \sin^2 i \cos \Psi - 2J \Psi \sin \Psi}{a^3\omega} & +\frac{2J \Psi \cos \Psi}{a^3\omega} & -\frac{2J \cos i \sin i \cos^2 \Psi}{a^3\omega} \\ (M-a)\omega \sin i \cos \Psi & (1 + \frac{\omega^2 a^2}{2} + \frac{M}{a}) \sin i \cos \Psi & (1 + \frac{M}{a}) \sin i \sin \Psi & -(1 + \frac{M}{a}) \cos i \\ & -\frac{2J \cos i \sin i \cos \Psi}{a^3\omega} & & -\frac{2J \sin^2 i \cos^2 \Psi}{a^3\omega} \end{pmatrix}. \quad (38)$$

Under such local frame, the tidal matrix $K_{(a)(b)}$ in Eq. (12) can be derived. As expected, up to the PN level the components $K_{(0)(a)} = 0$, and the Newtonian spatial part reads

$$(K^N)_{(i)(j)} = \begin{pmatrix} \frac{M}{a^3} & 0 & 0 \\ 0 & -\frac{2M}{a^3} & 0 \\ 0 & 0 & \frac{M}{a^3} \end{pmatrix} \quad (39)$$

which agrees exactly with the Newtonian tidal tensor $\partial_i \partial_j U$ evaluated in the LVLH frame along circular

orbits. The PN parts turns out to be

$$(K^{GE})_{(i)(j)} = \begin{pmatrix} -\frac{3M^2}{a^4} & 0 & 0 \\ 0 & \frac{3M(2M-a^3\omega^2)}{a^4} & 0 \\ 0 & 0 & -\frac{3M(M-a^3\omega^2)}{a^4} \end{pmatrix}, \quad (40)$$

$$(K^{GM})_{(i)(j)} = \begin{pmatrix} 0 & 0 & \frac{3J\omega \sin i \cos \Psi}{a^3} \\ 0 & \frac{6J\omega \cos i}{a^3} & -\frac{9J\omega \sin i \sin \Psi}{a^3} \\ \frac{3J\omega \sin i \cos \Psi}{a^3} & -\frac{9J\omega \sin i \sin \Psi}{a^3} & -\frac{6J\omega \cos i}{a^3} \end{pmatrix}. \quad (41)$$

V. Post-Newtonian Extension of Hill-Clohessy-Wiltshire Equations

Now, with all the results that gathered in previous sections, we substitute the orbit given in Eq. (24)-(28), the Christoffel symbols in Eq. (15)-(20), the tetrad matrices in Eq. (37) and (38), and the tidal matrices in Eq. (39) - (41) into the geodesic deviation equation (10). With straightforward but tedious algebraic manipulations and leaving out all the terms beyond $\frac{|Z|}{a^2}\mathcal{O}(\epsilon^4)$ and $\frac{|Z|}{a^2}\Psi\mathcal{O}(\epsilon^4)$, the geodesic deviation equation (10) under the local frame can be cast into an elegant form. Recovering the SI units, the final form of the Post-Newtonian extension of the Hill-Clohessy-Wiltshire equations along a relativistic nearly circular orbit turns out to be

$$\begin{aligned} & \begin{pmatrix} \ddot{Z}^{(1)}(\tau) \\ \ddot{Z}^{(2)}(\tau) \\ \ddot{Z}^{(3)}(\tau) \end{pmatrix} + \underbrace{\begin{pmatrix} 0 & 0 & 0 \\ 0 & -3\omega^2 & 0 \\ 0 & 0 & \omega^2 \end{pmatrix}}_{\text{Newtonian gradient}} \begin{pmatrix} Z^{(1)}(\tau) \\ Z^{(2)}(\tau) \\ Z^{(3)}(\tau) \end{pmatrix} + \underbrace{\begin{pmatrix} 0 & 2\omega & 0 \\ -2\omega & 0 & 0 \\ 0 & 0 & 0 \end{pmatrix}}_{\text{Coriolis}} \begin{pmatrix} \dot{Z}^{(1)}(\tau) \\ \dot{Z}^{(2)}(\tau) \\ \dot{Z}^{(3)}(\tau) \end{pmatrix} \\ & + \underbrace{\begin{pmatrix} 0 & 0 & \frac{4GJ\omega \sin i \cos(\tau\omega)}{c^2 a^3} \\ 0 & \frac{6a^2\omega^4}{c^2} - \frac{12GJ\omega \cos i}{c^2 a^3} & -\frac{10GJ\omega \sin i \sin(\tau\omega)}{c^2 a^3} \\ 0 & -\frac{12GJ\omega \sin i \sin(\tau\omega)}{c^2 a^3} & 0 \end{pmatrix}}_{\text{PN gradient}} \begin{pmatrix} Z^{(1)}(\tau) \\ Z^{(2)}(\tau) \\ Z^{(3)}(\tau) \end{pmatrix} \\ & + \underbrace{\begin{pmatrix} 0 & \frac{6GJ \cos i}{c^2 a^3} - \frac{3a^2\omega^3}{c^2} & \frac{4GJ \sin i \sin(\tau\omega)}{c^2 a^3} \\ \frac{3a^2\omega^3}{c^2} - \frac{6GJ \cos i}{c^2 a^3} & 0 & -\frac{2GJ \sin i \cos(\tau\omega)}{c^2 a^3} \\ -\frac{4GJ \sin i \sin(\tau\omega)}{c^2 a^3} & \frac{2GJ \sin i \cos(\tau\omega)}{c^2 a^3} & 0 \end{pmatrix}}_{\text{PN corrections to Coriolis}} \begin{pmatrix} \dot{Z}^{(1)}(\tau) \\ \dot{Z}^{(2)}(\tau) \\ \dot{Z}^{(3)}(\tau) \end{pmatrix} = 0, \end{aligned} \quad (42)$$

with the time component of the geodesic deviation equation (10) has the trivial form as expected

$$\ddot{Z}^0(\tau) = 0.$$

One notices that if all the PN corrections, that the second and the last lines of the above equation, are left out, the classical HCW equations, that the first line in the above equation, can be recovered. The second line in the above equation results from the combination of the PN tidal forces from spacetime curvature and the PN corrections to inertia forces caused by the geodetic [31] and Schiff [32] precessions of the local inertia frame along the orbit. The last line comes from the PN corrections to the Coriolis forces. Eq. (42) is the key result of this work, which may be taken as the foundation and starting point of the studies of relativistic dynamics of relative orbit motions.

As a demonstration of possible applications of the extended equations, we end up this section with the PN corrections to the general periodic solutions of the classical HCW equations

$$\begin{pmatrix} \ddot{Z}^{(1)}(\tau) \\ \ddot{Z}^{(2)}(\tau) \\ \ddot{Z}^{(3)}(\tau) \end{pmatrix} + \begin{pmatrix} 0 & 0 & 0 \\ 0 & -3\omega^2 & 0 \\ 0 & 0 & \omega^2 \end{pmatrix} \begin{pmatrix} Z^{(1)}(\tau) \\ Z^{(2)}(\tau) \\ Z^{(3)}(\tau) \end{pmatrix} + \begin{pmatrix} 0 & 2\omega & 0 \\ -2\omega & 0 & 0 \\ 0 & 0 & 0 \end{pmatrix} \begin{pmatrix} \dot{Z}^{(1)}(\tau) \\ \dot{Z}^{(2)}(\tau) \\ \dot{Z}^{(3)}(\tau) \end{pmatrix} = 0.$$

With the initial values $\{\dot{Z}^{(i)}(0) = \dot{Z}_0^{(i)}, Z^{(i)}(0) = Z_0^{(i)}\}$, the general solutions have the form

$$\begin{aligned} Z^{(1)}(\tau) &= Z_0^{(1)} + 6Z_0^{(2)}(\sin(\omega\tau) - \omega\tau) + \frac{4\dot{Z}_0^{(1)}\sin(\omega\tau)}{\omega} \\ &\quad - 3\dot{Z}_0^{(1)}\tau + \frac{2\dot{Z}_0^{(2)}(\cos(\omega\tau) - 1)}{\omega}, \\ Z^{(2)}(\tau) &= Z_0^{(2)}(4 - 3\cos(\omega\tau)) + \frac{2\dot{Z}_0^{(1)}(1 - \cos(\omega\tau))}{\omega} + \frac{\dot{Z}_0^{(2)}\sin(\omega\tau)}{\omega}, \\ Z^{(3)}(\tau) &= Z_0^{(3)}\cos(\omega\tau) + \frac{\dot{Z}_0^{(3)}\sin(\omega\tau)}{\omega}. \end{aligned}$$

To remove the drift terms we set $\dot{Z}_0^{(1)} = 0$ and $Z_0^{(2)} = 0$, and the general periodic solutions $Z_p^{(i)}(\tau)$ of the HCW equations read

$$Z_p^{(1)}(\tau) = Z_0^{(1)} + \frac{2\dot{Z}_0^{(2)}(\cos(\omega\tau) - 1)}{\omega}, \quad (43)$$

$$Z_p^{(2)}(\tau) = \frac{\dot{Z}_0^{(2)}\sin(\omega\tau)}{\omega}, \quad (44)$$

$$Z_p^{(3)}(\tau) = Z_0^{(3)}\cos(\omega\tau) + \frac{\dot{Z}_0^{(3)}\sin(\omega\tau)}{\omega}. \quad (45)$$

These solutions had already found many applications in the literature. For future SST missions and missions with high-precision optical gradiometers (as demonstrated in LPF), the PN corrections to

the above periodic solutions may be important to the measurements, especially to those in the along track direction. Let us assume the PN solutions to be $Z_P^{(i)}(\tau) + \delta^{(i)}(\tau)$ with $\delta^{(i)}(\tau) \sim |Z_P| \mathcal{O}(\epsilon^2)$ the PN corrections to the periodic solution given in Eq. (43)-(45). Substitute $Z_P^{(i)}(\tau) + \delta^{(i)}(\tau)$ into Eq. (42) and leaving out terms beyond $\frac{|Z_P|}{a^2} \mathcal{O}(\epsilon^4)$, we have

$$\begin{aligned} \ddot{\delta}^{(1)}(\tau) = & -2\omega\dot{\delta}^{(2)}(\tau) + \frac{3a^2\dot{Z}_0^{(2)}\omega^3}{c^2} \cos(\tau\omega) + \frac{4GZ_0^{(3)}J\omega \sin i \sin^2(\omega\tau)}{c^2a^3} \\ & - \frac{4GZ_0^{(3)}J\omega \sin i \cos^2(\omega\tau) + 6G\dot{Z}_0^{(2)}J \cos i \cos(\omega\tau)}{c^2a^3} \\ & - \frac{4G\dot{Z}_0^{(3)}J \sin i \sin(2\omega\tau)}{c^2a^3}, \end{aligned} \quad (46)$$

$$\begin{aligned} \ddot{\delta}^{(2)}(\tau) = & 3\omega^2\delta^{(2)}(\tau) + 2\omega\dot{\delta}^{(1)}(\tau) + \frac{4GZ_0^{(3)}J\omega \sin i \sin(2\omega\tau)}{c^2a^3} \\ & + \frac{10G\dot{Z}_0^{(3)}J \sin i \sin^2(\omega\tau)}{c^2a^3} + \frac{2G\dot{Z}_0^{(3)}J \sin i \cos^2(\omega\tau)}{c^2a^3}, \end{aligned} \quad (47)$$

$$\ddot{\delta}^{(3)}(\tau) = -\omega^2\delta^{(3)}(\tau) - \frac{GJ\dot{Z}_0^{(2)} \sin i (3 \cos(2\omega\tau) - 1)}{c^2a^3}. \quad (48)$$

With the initial conditions $\{\delta_0^{(i)} = \dot{\delta}_0^{(i)} = 0\}$, the general solutions can be worked out as

$$\begin{aligned} \delta^{(1)}(\tau) = & \frac{3a^2\dot{Z}_0^{(2)}\omega}{c^2} (2\tau\omega \sin(\omega\tau) + 3 \cos(\omega\tau) - 3) \\ & - \frac{6G\dot{Z}_0^{(2)}J \cos i (2\tau\omega \sin(\omega\tau) + 3 \cos(\omega\tau) - 3)}{c^2a^3\omega^2} \\ & + \frac{GZ_0^{(3)}J \sin i (\cos(2\omega\tau) - 1)}{c^2a^3\omega} \\ & + \frac{G\dot{Z}_0^{(3)}J \sin i (4 \sin(\omega\tau) + \sin(2\omega\tau) - 6\tau\omega)}{c^2a^3\omega^2}, \end{aligned} \quad (49)$$

$$\begin{aligned} \delta^{(2)}(\tau) = & -\frac{3a^2\dot{Z}_0^{(2)}\omega}{c^2} (\tau\omega \cos(\omega\tau) - \sin(\omega\tau)) \\ & - \frac{6G\dot{Z}_0^{(2)}J \cos i (\sin(\omega\tau) - \tau\omega \cos(\omega\tau))}{c^2a^3\omega^2} \\ & - \frac{2G\dot{Z}_0^{(3)}J \sin i (\cos(\omega\tau) - 1)}{c^2a^3\omega^2}, \end{aligned} \quad (50)$$

$$\delta^{(3)}(\tau) = -\frac{4G\dot{Z}_0^{(2)}J \sin i \sin^2\left(\frac{\omega\tau}{2}\right) \cos(\omega\tau)}{c^2a^3\omega^2}. \quad (51)$$

There exist a drift term in $\delta^{(1)}(\tau)$ in the last line of Eq. (49), which may be further removed by assuming $\dot{Z}_0^{(3)} = 0$. The solutions also contain oscillating terms with growing magnitudes in $\delta^{(1)}(\tau)$ and $\delta^{(2)}(\tau)$ within the $e_{(1)}^\mu - e_{(2)}^\mu$ plane (the orbital plane), which remain true only when the conditions $|\delta^{(i)}(\tau)| \ll |Z_p|$ are satisfied. For applications, even after $\frac{\tau\omega}{2\pi} \sim 10^4$ orbital cycles, one has the magnitudes estimation $|\delta^{(i)}(\tau)| \sim |Z_p| \tau\omega \mathcal{O}(\epsilon^2) \leq 10^{-6} \times |Z_p|$, and still these solutions can be taken as good approximations.

VI. Conclusions

This work can be viewed as the first-step study of the relativistic dynamics of relative orbit motions. A systematic approach to the linearized theory through the geodesic deviation equation in GR is introduced. When the centered source is modeled as an ideal uniform and rotating spherical body, the relativistic equations, that Eq. (42), determining the relative motions with respect to a relativistic circular orbit are derived up to the PN level. These equations are the PN extensions of the classical HCW equations, which may be taken as the starting point for future studies of relativistic relative orbit motions. The PN corrections given in Eq. (49)-(51) to the periodic solutions of the HCW equations, especially the growing oscillating terms, show that general relativistic effects may be important to both inter-satellites ranges measurements and space-borne gradient measurements. While, for practical applications of the generalized HCW equations to such problems, one needs to work with the much more complicated metric given in Eq. (8) to enclose perturbations from certain geopotential multipoles, choose a more accurate reference orbit and deal with the related errors in a more sophisticated way. Such topics, as natural subsequent works, will be left for future studies.

Acknowledgments

Supports from National Space Science Center, Chinese Academy of Sciences (No. XDA04077700), National Natural Science Foundation of China (No. 11171329 and No. 41404019) and Central Universities Funds (No. 2014G3262010 and No. 310826161010) are acknowledged. We are grateful to Yun Kau Lau for initiating the study of the problem and encouraging us to do this work. The author Peng Xu is also grateful to Shing-Tung Yau for his continuous support at the Morningside Center of Mathematics, Chinese Academy of Sciences. Valuable discussions with Dr. Wenlin Tang is acknowledged.

References

- [1] Clohessy, W. H. and Wiltshire, R. S., "Terminal Guidance System for Satellite Rendezvous," *Journal of the Aerospace Sciences*, Vol. 27, No. 9, 1960, pp. 653-658.
- [2] Hill, G. W., "Researches in the Lunar Theory," *American Journal of Mathematics*, Vol. 1, No. 1, 1878, pp. 5-26.

- [3] Schrama, E. J. O., “The Role Of Orbit Errors In Processing Of Satellite Altimeter Data,” Ph.D. Dissertation, Delft University Of Technology, Netherlands, 1989.
- [4] Colombo, O. L. and Maryland, M., “The Dynamics Of Global Positioning System Orbits And The Determination Of Precise Ephemerides,” *Journal of Geophysical Research*, Vol. 94, No. B7, 1989, pp. 9167-9182.
- [5] Schrama, E. J. O., “Gravity Field Error Analysis: Applications of Global Positioning System Receivers and Gradiometers on Low Orbiting Platforms,” *Journal of Geophysical Research*, Vol. 96, No. B12, 1991, 20041-200051.
- [6] Sneeuw, N., “Global Gravity Field Error Simulations for STEP-Geodesy,” *A Major STEP for Geodesy*, edited by R. Rummel and P. Schwintzer, GFZ Potsdam, Germany, Nov. 1994, pp. 45-54.
- [7] Wolff, M., “Direct measurements of the earth’s gravitational potential using a satellite pair,” *Journal of Geophysical Research*, Vol. 74, 1969, pp. 5295-5300.
- [8] Colombo, O. L., *The Global Mapping of Gravity with Two Satellites*, Publications on Geodesy, New Series, Vol. 7, No. 3, Netherlands Geodetic Commission, 1984.
- [9] Colombo, O. L., “Notes on the Mapping of the Gravity Field using Satellite Data,” *Mathematical and Numerical Techniques in Physical Geodesy*, edited by H. S’unkel, Lecture Notes in Earth Sciences, Vol. 7, Springer-Verlag, Berlin, 1986.
- [10] R. Mackenzie, R. and Moore, P., “A geopotential error analysis for a non planar satellite to satellite tracking mission,” *Journal of Geodesy*, Vol. 71, 1997, pp. 262-272.
- [11] Sneeuw, N., “A Semi-Analytical Approach to Gravity Field Analysis from Satellite Observations,” Ph.D. Dissertation, Fakultät für Bauingenieur-und Vermessungswesen, Technischen Universität München, 2000.
- [12] Armano, M., et al., “Sub-Femto-g Free Fall for Space-Based Gravitational Wave Observatories: LISA Pathfinder Results,” *Physical Review Letters*, Vol. 116, 2016, 231101.
- [13] Xu, P., et al., “Precision measurement of planetary gravitomagnetic field in general relativity with laser interferometry in space — Theoretical foundation,” *submitted for publication*.
- [14] Iorio, L., “Dynamical orbital effects of general relativity on the satellite-to-satellite range and range-rate in the GRACE mission: A sensitivity analysis,” *Advances in Space Research*, Vol. 50, 2012, pp. 334-345.
- [15] Qiang, L.-E. and Xu, P., “Signature of biased range in the non-dynamical Chern-Simons modified gravity and its measurements with satellite-satellite tracking missions: theoretical studies,” *The European Physical Journal C*, Vol. 75, 2015, 390.

- [16] Mashhoon, B., Paik, H. J., and Will, C. M., “Detection of the gravitomagnetic field using an orbiting superconducting gravity gradiometer. Theoretical principles,” *Physical Review D*, Vol. 39, 1989, pp. 2825-2838.
- [17] Qiang, L.-E. and Xu, P., “Testing Chern-Simons modified gravity with orbiting superconductive gravity gradiometers: the non-dynamical formulation,” *General Relativity and Gravitation*, Vol. 47, 2015, 26.
- [18] Qiang, L.-E. and Xu, P., “Probing the post-newtonian physics of semi-conservative metric theories through secular tidal effects in satellite gradiometry missions,” *International Journal of Modern Physics D*, Vol. 25, No. 6, 2016, 1650070.
- [19] Will, C. M., *Theory and experiment in gravitational physics*, Cambridge University Press, 1993.
- [20] Will, C. M., “The Confrontation between General Relativity and Experiment,” *Living Reviews in Relativity*, Vol. 17, 2014, 4.
- [21] Abbott, B. P., et al., “GW150914: The Advanced LIGO Detectors in the Era of First Discoveries,” *Physical Review Letters*, Vol. 116, 2016, 131103.
- [22] Turyshev, S. G., “Experimental Tests of General Relativity,” *Annual Review of Nuclear and Particle Science*, Vol. 58, 2008, pp. 207-248.
- [23] Weinberg, S., *Gravitation and Cosmology: Principles and Applications of the General Theory of Relativity*, Wiley, New York, 1972.
- [24] Straumann, N., *General relativity and relativistic astrophysics*, Springer-Verlag, Berlin, 1984.
- [25] Wald, R. M., *General Relativity*, University of Chicago Press, Chicago, 1984.
- [26] Ni, W.-T., and Zimmermann, M., “Inertial and gravitational effects in the proper reference frame of an accelerated, rotating observer,” *Physical Review D*, Vol. 17, 1978, pp. 1473-1476.
- [27] Thorne, K. S., “Gravitomagnetism, jets in quasars, and the Stanford Gyroscope Experiment,” *Near Zero: New Frontiers of Physics*, edited by Fairbank, J. D., Deaver Jr., B. S., Everitt, C. W. F., and Michelson, P. F., Elsevier, New York, 1988, pp. 573-586.
- [28] Ciufolini, I., and Wheeler, J. A., *Gravitation and Inertia*, Princeton University Press, Princeton, 1995.
- [29] Maartens, R., and Bassett, B. A., “Gravitoelectromagnetism,” *Classical Quantum Gravity*, Vol. 15, 1998, pp. 705-717.
- [30] Lense, J., and Thirring, H., “Ueber den Einfluss der Eigenrotation der Zentralkörper auf die Bewegung der Planeten und Monde nach der Einsteinschen Gravitationstheorie,” *Z. Phys.*, Vol. 19, 1918, pp. 156-163.
- [31] de Sitter, W., “Einstein’s theory of gravitation and its astronomical consequences,” *Monthly Notices of the Royal Astronomical Society, First Paper*, Vol. 76, 1916, pp. 699-728.

- [32] Schiff, L. I., “Motion of a Gyroscope According to Einstein’s Theory of Gravitation,” *Proceedings of the National Academy of Sciences*, Vol. 46, 1960, pp. 871-882.